Desalination and Water Treatment
www.deswater.com
1944-3994/1944-3986 © 2012 Desalination Publications. All rights reserved
doi: 10/5004/dwt.2012.3184

Taylor & Francis
Taylor & Francis Group

45 (2012) 84–90
July

Modification of polyamide membrane surface with chlorine dioxide solutions of differing pH

Erewari Alayemieka[a,b], SeockHeon Lee[b,*]

[a]*Department of Construction and Environment Engineering, University of Science and Technology, Deajeon, 113 Gwahangno, Yuseong-gu, Deajeon, Republic of Korea*
[b]*Water Resource Center, Korea Institute of Science and Technology, Hwarangno 14-gil 5, Seongbuk-gu, Seoul 136-791, Republic of Korea*
Tel. +82 2 958 6644; Fax: +82 2 958 5839; email: seocklee@kist.re.kr

Received 8 August 2011; Accepted 13 November 2011

ABSTRACT

Free chlorine is the common biocide used in the membrane desalination industry. However, it is incompatible with polyamide membranes. Chlorine dioxide (ClO_2) is an effective biocide and is more compatible with polyamide membranes. The effects of ClO_2 on polyamide membrane hydrophillicity and surface charge were studied under static soaking conditions. Membrane coupons were soaked in acidic, neutral, and alkaline pHs of ClO_2. The membrane's hydrophilicity and surface charge were assessed by dynamic contact angle and streaming potential analyzer respectively, while performance was analyzed on a bench scale desalination system. The result of the experiment showed that ClO_2 influenced membrane hydrophilicity and surface charge. Hydrophilicity improved irrespective of ClO_2 pH, whereas surface charge was either suppressed or improved depending on ClO_2 pH. Permeate flux increased for acidic, neutral, and alkaline conditions by 34%, 34%, and 77%, respectively. A slight trade-off in salt leakage for acidic and alkaline pH conditions was observed. The phenomenal performance of ClO_2 oxidized membrane was influenced by modifications in both the membrane surface and chemical characteristics.

Keywords: Polyamide membrane; Oxidation; Chlorine dioxide pH; Surface properties modification; Membrane selectivity; Membrane permeate

1. Introduction

Sea and brackish water inevitably contain organics and microorganisms that make membrane desalination systems vulnerable to biofouling. Pretreatment units designed to remove organics and inactivate microorganisms are therefore integral parts of desalination systems. Free chlorine is the common microorganism inactivator in the industry. However, its residual effect degrades polyamide (PA) membrane performance [1–7].

PA is the widely accepted thin film composite (TFC) membrane material type with high thermal, chemical, and hydrolytic stability. Its incompatibility with free chlorine necessitates the search for alternate disinfectants. Chlorine dioxide (ClO_2) and monochloramines (MCA) have been reported to be less aggressive to PA [8–10]. Although MCA is less aggressive than ClO_2, ClO_2 is preferred as an alternate disinfectant because of its enormous sterling properties. ClO_2 is more effective as a biocide than MCA. Unlike MCA, ClO_2 is permeable through RO membrane [8] preventing its accumulation on membrane surface. MCA reacts with bromine to form

*Corresponding author.

bromate and bromide, which are both carcinogenic and difficult to remove by RO membranes [11,12].

The lower aggressiveness of ClO_2 was assessed with membrane performances (salt rejection and permeate flux) based on the extent of modification of the membranes' chemical structures. However, membrane performance is also influenced by membrane surface characteristics such as hydrophillicity and surface charge. These are effects of highly active end groups of the polyamide molecule that can participate in chain/radical interactions. Several workers have taken advantage of the high reactivity of the end groups and modified surface properties of commercial PA membranes through free radical grafting of monomers and plasma treatment [13–23]. Interestingly, oxygen plasma treatment and grafting with hydroxyl moieties are similar to the oxidative radical coupling mechanism. Hence, like surface modification techniques, oxidative radical coupling in polyamide should have a synergistic effect on the performance of membranes. This work, therefore, elucidates the effect of ClO_2 pH on the surface characteristics and performance of a polyamide membrane.

2. Materials and methods

2.1. Preparation of chlorine dioxide solutions and the oxidation of a polyamide membrane

ClO_2 stock solution was prepared by acidifying sodium chlorite ($NaClO_2$) solution with sulfuric acid (H_2SO_4), as shown in Eq. (1). A given quantity of dilute H_2SO_4 was slowly added to $NaClO_2$ in intervals of 5 min while a smooth current of air passed through the system. Generated ClO_2 gas was passed through a saturated $NaClO_2$ solution for purification. Pure ClO_2 gas was collected in deionized water in a steady stream of air. This preparation method was carried out according to the description of Standard Methods for the Examination of Water and Wastewater (1998) 4500-ClO_2B with slight modification involving the immersion of the gas collecting bottle in an ice bath for higher gas solubility. The ClO_2 stock solution was placed in a dark brown glass container and stored at 4°C. The concentration of the ClO_2 solution was directly measured using a spectrophotometer (DR 5000, HACH, USA). This is a standard *N,N*-diethly-*p*-phenylenediamine (DPD) color change method according to the description of Standard Methods for the Examination of Water and Wastewater (1998) (4500-ClO_2 D):

$$4NaClO_2 + 2H_2SO_4 \rightarrow 2ClO_2 + HCl + HClO_3 + 2Na_2SO_4 + H_2O \quad (1)$$

Membrane coupons cut from commercial spiral wound membrane (TM820H-400, Toray—Japan) were immersed in buffered ClO_2 solutions of pH 4, 7, and 9 for a contact time of 100 ppm h (20 ppm × 5 h). Membrane characteristics as described by the manufacturer are shown in Table 1. The membrane oxidation unit was kept in a dark hood throughout the oxidation time (5 h), and the experiment was repeated with several membrane coupons to ensure reproducibility. At the end of the membrane soaking period, the concentration of ClO_2 declined from 20 ppm to 5 ppm for all pH conditions, indicating the reduction of ClO_2. Eqs. (2) and (3) are the step-wise redox equations:

Step 1:

$$ClO_{2(aq)} + e^- \rightarrow ClO_2^- \qquad E = 0.954\ V \quad (2)$$

Step 2:

$$ClO_2^- + 4H^+ + 4e^- \rightarrow Cl^- + 2H_2O \qquad E = 0.76\ V \quad (3)$$

2.2. Membrane performance test

NaCl solution of 5000 ppm was filtered using a batch type concentrate-3-stage RO test stand, as shown in Fig. 1. Each stage was designed with two circular symmetrical steel parts with an effective membrane area of 2.275×10^3 mm^2. The membrane compartment was furnished with a permeate port, allowing the permeate flow to exit the membrane unit. In addition, a resistant compact O-ring and stainless steel sintered mesh were in place to prevent membrane displacement and deformation. The test stand was operated at a pressure of 49 bar in a cross-flow configuration of 3 l min^{-1}. Other integral parts of the test

Table 1
Membrane characteristics as outlined by manufacturers

Membrane characteristics	Toray
Maximum operating pressure	5.5 MPa
Maximum feed water temperature	45°C
Feed water chlorine concentration	Not detectable
Maximum feed water silt density index	5
Feed water pH range, continuous operation	2–11
Feed water pH range, chemical cleaning	1–12

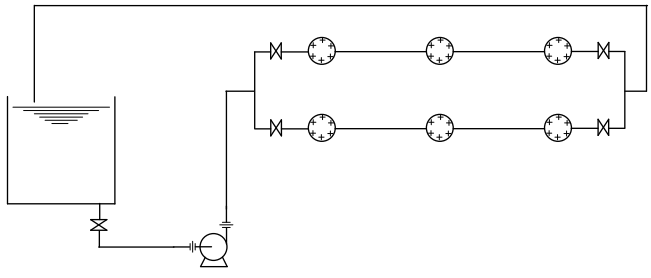

Fig. 1. Schematic diagram of the RO test rig.

stand included a feed tank, a water cooler, pumps, and a control unit. The water cooler automatically regulated the feed stream temperature to maintain a temperature of 25°C. Membrane performances were assessed with respect to permeate flux and salt rejection. For ease of identification of the membranes oxidized at pHs of 4, 7, and 9 buffered ClO_2 solutions, membranes were labeled as T-acidic, T-neutral, and T-alkaline respectively. The unoxidized membrane was labeled as T-membrane.

2.3. Characterization of membrane hydrophilicity and surface charge

Membrane hydrophilicity was assessed with a dynamic contact angle. A dynamic contact angle was determined based on the Wilhelm plate method. Measurements were carried out using a Sigma 701 microbalance (KSV Instrument, Ltd., Finland) interfaced with a PC for automatic control and data acquisition. During the measurement, a membrane sample was held in a vertical position by the automated microbalance. A liquid cell containing the deionized water moved up and down at constant speed. The sample was then pushed into or pulled out of the deionized water by the automated microbalance. The surface tension of test liquids was measured at each time by the Force Du Nouy ring method at room temperatures of 28≈29°C with a humidity of 60–65%. The ring was rinsed with ethyl alcohol prior to the measurement.

Surface charge density characterization was accomplished with a Surpass streaming potential analyzer (Anton Paar GmbH, Austria). A 1 mM KCl electrolyte solution was used as the background solution for analysis. The background solution pH was adjusted within the range of 3≈10 by the addition of small amounts of HCl or NaOH. Prior to analysis, the inner part of the instrument was rinsed with deionized water. Streaming potential was measured at regulated pressures within the range of 0–500 mbar. Temperature was maintained between 24°C and 25°C. Zeta potential was calculated from the measured streaming potential using the Fairbrother and Mastin substitution.

2.4. Membrane molecular structure analysis

Assessment of the sample-membranes' molecular structures was made using Time-of-Flight Secondary Ion Mass Spectrometry (TOF-SIMS) and X-ray photoelectron spectroscopy (XPS). TOF-SIMS (IONTOF, Germany) probes were set at a short distance of 1–10 Å into the membrane surface. The spectra were devoid of substrate layer interference. Analyses were performed under static conditions with a Cesium ion (Cs^+) gun of 1 nA ion current and a low beam voltage of 8 eV. The TOF-SIMS spectra of secondary ions were obtained over a mass range of 0–400 in positive mode. However, the analysis of the polyamide structure was achieved by the appropriate selection of ions within the lower mass ions ($m/z < 100$) using formulae for the common ion series of $C_nH_{2n}N^+$, $C_nH_{2n+2}N^+$, $C_nH_{2n+2}NCO^+$, $C_nH_nO_2^+$, and $C_{2n}H_{2n+2}O_2^+$. These series are descriptive of the highly active amine and carboxylic end groups as well as amide bonds. For the aromatic hydrocarbon chain integrity, $C_nH_n^+$ ion series with n starting from six was employed. The selection of lower mass ions ($m/z < 100$) gives fewer possible ion assignments for a particular mass value. Furthermore, low-mass ions produce much more complete homologous series and much less difference in ion abundance than higher masses.

XPS (PHI-5800 ESCA spectrometer, ULVAC-PHI, Paris) with a monochromated aluminum Kα? as its X-ray source (hv = 1486.6 eV) was operated at a power of 250 W and a background pressure of 2×10^{-10} Torr. Its beam energy, filament current, and carbon C (1s) binding energy were 10 kV, 27 nA, and 284.6 respectively. The sampling depth of 10 nm was obtained with a spectra electron emission angle of 45°. The effect of surface irregularity was removed using a large spot size of 400 µm × 400 µm. Spectra resolution was maximized by the application of surface charge neutralization systems.

3. Results

3.1. Effect of ClO_2 on PA membrane surface charge and hydrophilicity

The effect of ClO_2 on membrane surface charge characteristics are displayed in Fig. 2. The unoxidized membrane (T-membrane) possessed positive and negative charges. These, according to the membrane elemental composition in Table 2, are products of protons transfer in amine and carboxylic end groups. In aqueous solution of

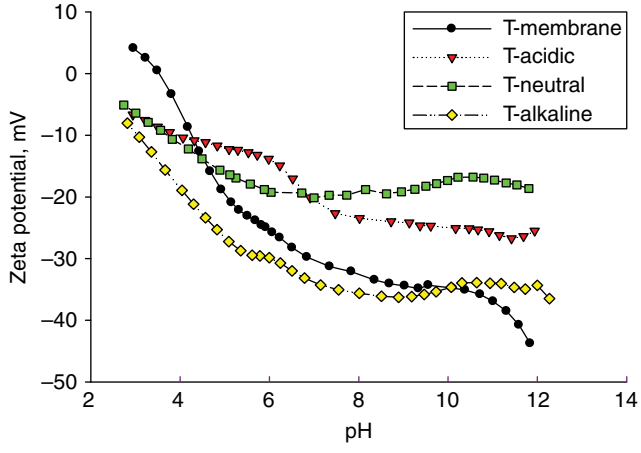

Fig. 2. Surface charge density of unoxidized and oxidized membrane.

Table 2
Membrane relative atomic concentration and atomic concentration ratio

Membranes	C%	N%	O%	S%	Cl%
T-membrane	70.83	9.65	17.49	0.44	1.59
T-acidic	70.19	10.54	17.38	0.23	1.66
T-neutral	71.28	9.94	17.11	0.17	1.50
T-alkaline	66.47	8.38	24.21	0.08	0.86

pH less than 3.5, the amine end group protonated (amine groups, $NH_2 \rightarrow NH_3^+$) to give positive charges, while at pH values above 3.5, the carboxylic group deprotonated (COOH→COO) to give negative charges. Upon exposure to ClO_2 solutions at pHs of 4 and 7, membrane surface charges (both positive and negative) were suppressed while, in alkaline solution (pH 9), only positive charges were suppressed and the negative charges improved. On the other hand, ClO_2 enhanced hydrophilicity despite the pH. The characteristic hydrophilicity and surface charge at pH 7 are summarized in Table 3.

3.2. Performance of unoxidized and oxidized membranes

Exposure of the PA membrane to ClO_2 solutions at pHs of 4 and 9 improved water permeability by 34% and 77%, respectively, while salt rejection decreased by 1.0% and 1.5%, respectively (Table 3). For membrane ClO_2 solutions at pH 7, permeability improved by 34% without any noticeable salt leakage.

4. Discussion

4.1. Effect of end group/chain interaction on surface charge

In the redox reaction, ClO_2 accepted electrons while the polyamide molecule eliminated the hydrogen atom, forming a series of radicals (Eqs. (4)–(8)). These radicals underwent a whole suit of reactions forming end groups with stabilized H-bonds (Eqs. (4) and (5)). The degree of stability was dependent on the pH of ClO_2.

Table 3
Membranes' surface characteristics and performance

Membrane	Zeta potential at pH 7 (mV)	Water contact angle (°)	Permeate flux ($l\ m^{-2}.h$)	Salt rejection (%)
T-membrane	–30	51	439.491	99.46
T-acidic	–19	39	588.265	98.47
T-neutral	–19	47	587.462	99.39
T-alkaline	–34	45	779.308	97.97

For pHs of 4 and 7, the highly reactive amine and carboxyl radicals interacted to form H-bonds too stable for dissociation (Eqs. (7) and (8)), suppressing both positive and negative charges. For pH 9, only amine radical interaction formed stable H-bonds that suppressed positive charges. The improvement of the negative charges was attributed to the disproportion of ClO_2 in base, as seen in Eqs. (9)–(11):

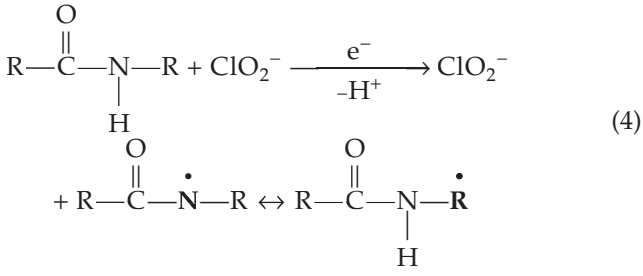

(4)

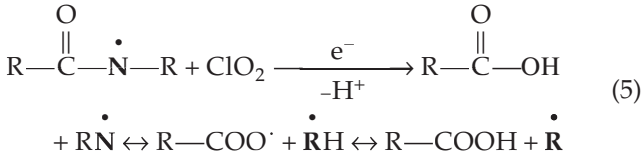

(5)

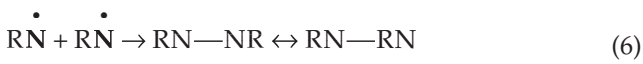

(6)

(7)

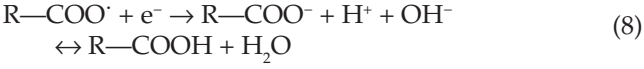

(8)

At alkaline pH, ClO_2 disproportionates to chlorite (ClO_2^-) and chlorate (ClO_3^-). Chlorate reduces to chlorite by the acceptance of two electrons while chlorite is further reduced to chloride by the acceptance of four electrons. However, the reduction potential of chlorate (0.33 V) is smaller than chlorite (0.76 V) and chlorine dioxide (0.954 V). Hence, the ease of the reduction of chlorate to chlorite makes Eq. (8) the predominate equation, leading to the formation of more carboxylate ($RCOO^-$), which improved the negative charge density:

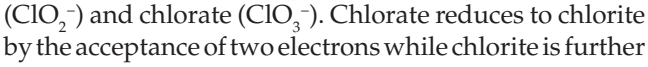

(9)

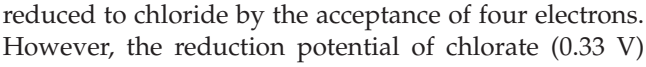

(10)

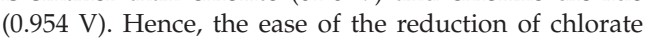

(11)

The degree of intramolecular hydrogen bond stability with respect to oxidation pH was revealed in the sum of nitrogenous and oxygenated ion species of TOF-SIMS spectra. TOF-SIMS ion intensities are a function of

H-bond strength. High ion intensity implies less resistance to the fragmentation of molecular and secondary ions and vice versa. The data in Table 4 shows that ClO_2 stabilized H-bonds of the carboxylic end groups for all pH conditions. However, at low pH (acidic range), the oxidative capacity of ClO_2 is high (Eq. (12)). Obviously, more radicals were formed in T-acidic, but this also implies more radical/chain interactions accompanied with amide and aromatic bond weakening. The higher sum of nitrogenous and hydrocarbon ion for T-acidic (Tables 5 and 6) expresses the weakened amide and aromatic bonds. The weakening of the amide and aromatic bond affected the carboxylic end groups, thereby increasing the sum of the oxygenated species of T-acidic more than T-neutral, giving the trend as T-membrane<T-alkaline<T-acidic<T-neutral (Table 4).

$$ClO_2 + 4H^+ + 5e = Cl^- + 2H_2O \quad (12)$$

As pH increased from the acidic to neutral range, the oxidative capacity of ClO_2 was lowered and the amide and aromatic bond strengths were stabilized. An increase in pH to the alkaline range further strengthens these bonds, giving the trend of the sum of the nitrogenous and hydrocarbon species as T-acidic<T-membrane≅ T-neutral<T-alkaline.

Table 4
Ion intensity of oxygenated species of oxidized and unoxidized polyamide membranes

Center mass	Assignment	Norm. by total ion mass intensity			
		T-membrane	T-acidic	T-neutral	T-alkaline
45	CHO_2^+	9.59×10^{-3}	2.56×10^{-3}	2.49×10^{-3}	6.53×10^{-3}
58	$C_2H_2O_2^+$	1.11×10^{-3}	4.29×10^{-4}	3.51×10^{-4}	7.04×10^{-4}
60	$C_2H_4O_2^+$	5.80×10^{-4}	1.78×10^{-4}	1.58×10^{-4}	3.33×10^{-4}
71	$C_3H_3O_2^+$	2.25×10^{-3}	6.56×10^{-4}	5.55×10^{-4}	1.67×10^{-3}
84	$C_4H_4O_2^+$	7.57×10^{-4}	4.47×10^{-4}	3.03×10^{-4}	3.86×10^{-4}
86	$C_4H_6O_2^+$	2.73×10^{-4}	1.13×10^{-4}	8.91×10^{-5}	1.62×10^{-4}
97	$C_5H_5O_2^+$	7.38×10^{-4}	3.39×10^{-4}	2.63×10^{-4}	6.33×10^{-4}
Σ	–	1.53×10^{-2}	4.72×10^{-3}	4.21×10^{-3}	1.04×10^{-2}

Table 5
Ion intensity of nitrogenous species of oxidized and unoxidized polyamide membranes

Center mass	Assignment	Norm. by total ion mass intensity			
		T-membrane	T-acidic	T-neutral	T-alkaline
28	CH_2N^+	8.66×10^{-3}	7.62×10^{-3}	7.49×10^{-3}	7.35×10^{-3}
30	CH_4N^+	5.09×10^{-3}	7.42×10^{-3}	6.06×10^{-3}	5.03×10^{-3}
42	$C_2H_4N^+$	3.66×10^{-3}	3.88×10^{-3}	3.24×10^{-3}	2.43×10^{-3}
44	$C_2H_6N^+$	3.28×10^{-4}	5.50×10^{-4}	2.96×10^{-4}	3.68×10^{-4}
56	$C_3H_6N^+$	2.08×10^{-3}	3.70×10^{-3}	2.47×10^{-3}	1.25×10^{-3}
58	$C_3H_8N^+/CH_4NCO^+$	1.99×10^{-3}	2.39×10^{-3}	1.73×10^{-3}	1.38×10^{-3}
70	$C_4H_8N^+$	2.88×10^{-3}	3.03×10^{-3}	1.63×10^{-3}	1.07×10^{-3}
72	$C_4H_{10}N^+/C_2H_6NCO^+$	1.02×10^{-3}	1.37×10^{-3}	9.35×10^{-4}	6.86×10^{-4}
84	$C_5H_{10}N^+$	7.57×10^{-4}	4.42×10^{-4}	3.03×10^{-4}	3.86×10^{-4}
86	$C_5H_{12}N^+/C_3H_8NCO^+$	4.47×10^{-4}	5.71×10^{-4}	3.95×10^{-4}	2.87×10^{-4}
98	$C_6H_{12}N^+$	4.23×10^{-4}	4.09×10^{-4}	2.83×10^{-4}	2.14×10^{-4}
100	$C_6H_{14}N^+/C_4H_{10}NCO^+$	79.12×10^{-4}	7.79×10^{-4}	1.65×10^{-3}	1.75×10^{-3}
Σ	–	2.87×10^{-2}	3.26×10^{-2}	2.67×10^{-2}	2.25×10^{-2}

Table 6
Ion intensity of hydrocarbon species of oxidized and unoxidized polyamide membranes

Center mass (m/z)	Assignment	Norm. by total ion mass intensity			
		T-membrane	T-acidic	T-neutral	T-alkaline
78	$C_6H_6^+$	1.94×10^{-3}	2.15×10^{-3}	2.05×10^{-3}	1.77×10^{-3}
91	$C_7H_7^+$	3.79×10^{-3}	4.73×10^{-3}	3.88×10^{-3}	3.88×10^{-3}
Σ	–	5.73×10^{-3}	6.88×10^{-3}	5.93×10^{-3}	5.65×10^{-3}

4.2. Effect of end group/chain interaction on hydrophilicity

As displayed in Table 3, the contact angle of the membrane declined from 51° with oxidation in acidic, neutral, and alkaline solutions to 39°, 47° and 45°, respectively. The sum of nitrogenous and oxygenated ion intensities of the unoxidized membrane (0.44) also decreased to 0.37, 0.31, and 0.33 for these membranes. This trend reveals the effect of both H-bond stability and the number of hydrogen bond sites in membrane surface hydrophilicity. The greater the number of hydrogen bond sites, the more hydrophilic the membrane.

4.3. Impact of membrane morphology on membrane performance

The characteristic permeate flux of the oxidized membrane correlates with improved hydrophilicity as well as operational conditions, such as applied pressure. The T-acidic membrane with better hydrophilicity showed the least flux while the T-alkaline membrane showed the highest flux. The weakened amide and aromatic bonds of T-acidic could have experienced compaction due to the high applied pressure (49 bar), which restricted water and salt passage, as in the work by Kwon et al. [2]. On the other hand, for T-alkaline and T-neutral membranes without considerable amide and aromatic bond weakening, the greater hydrophilic chain length of T-alkaline created free volume for both salt and water passage, similar to the work by Manttarri et al. [24]. T-neutral improved water permeability without any notable trade off on salt rejection.

5. Conclusions

The alteration of membrane surface properties is dependent on the pH of ClO_2. In this study, the hydrophilicity of the polyamide membrane improved for the three pH levels of ClO_2. ClO_2 suppressed positive charges in all pH range. Negative charges were suppressed at acidic and neutral pHs but improved at alkaline pH. Modification of the surface characteristics was influenced by end group H-bond stability and the number of hydrogen bond sites. The interaction of oxidative radicals produced end groups with stable H-bonds. Amine radical interaction was similar at all pHs, while the carboxyl radical interaction was slightly different at alkaline pH.

Membranes performances were influenced by membrane surface and chemical characteristics as well as applied pressure. Higher oxidative capacity of ClO_2 with acidity creates weak aromatic and amide bonds that are compacted with applied pressure, restricting salt and water permeability. Increased hydrophilic chain length increased the membrane free volume. The effect of ClO_2 on the membrane contact angle was comparably more significant than free volume. Hence, permeate flux improved with slight salt leakage.

Acknowledgements

This research was supported by a grant (07Seahero-B01–02) from the Plant Technology Advancement Program funded by the Ministry of Land, Transport, and Maritime Affairs of the South Korean government.

References

[1] N.P. Soice, A.R. Greenberg, W.B. Krantz and A.D. Norman, Studies of oxidative degradation in polyamide RO membranes barrier layers using pendant drop mechanical analysis, J. Membr. Sci., 243 (2004) 345–355.
[2] Y.-N. Kwon and J.O. Leckie, Hypochlorite degradation of cross linked polyamide membranes. I. Changes in chemical/morphological properties, J. Membr. Sci., 283 (2006) 21–26.
[3] A. Antony, R. Fudianto, S. Cox and G. Leslie, Assessing the oxidative degradation of polyamide reverse osmosis membrane-accelerated ageing with hypochlorite exposure, J. Membr. Sci., 347 (2010) 159–164.
[4] J. Glater, S. Hong and M. Elimelech. The search for a chlorine-resistant reverse osmosismembrane, Desalination, 95 (1994) 325–345.
[5] S. Wu, J. Xing, G. Zheng, H. Lian and L. Shen, Chlorination and oxidation of aromatic polyamides I1. Chlorination of some aromatic polyamides, J. Appl. Polym. Sci., 61 (1996) 1305–1314.
[6] S. Wu, G. Zheng, H. Lian, J. Xing and L. Shen, Chlorination and oxidation of aromatic polyamides I. Synthesis and characterization of some aromatic polyamides, J. Appl. Polym. Sci., 61 (1996) 415–420.
[7] G.-D. Kang, C.-J. Gao, W.-D. Chen, X.-M. Jie, Y.-M. Cao and Q. Yuan, Study on hypochlorite degradation of aromatic polyamide reverse osmosis membrane, J. Membr. Sci., 300 (2007) 165–171.

[8] W.R. Adam, The effects of chlorine dioxide on reverse osmosis membrane, Desalination, 78 (1990) 439–453.
[9] J. Glater, M.R. Zachariah, S.B. McCray and J.W. McCutchan, Reverse osmosis membrane sensitivity to ozone and halogen disinfectants, Desalination, 48 (1983) 1–16.
[10] K.M. Silva, C.I. Tessaro and K. Wada, Investigation of oxidative degradation of polyamide reverse osmosis membranes by monochloroamine solution, J. Membr. Sci., 282 (2006) 375–382.
[11] M. Belluati, E. Danesi, G. Petrucci and M. Rosellini, Chlorine dioxide disinfection technology to avoid bromated formation in desalinated seawater in potable waterworks, Desalination, 203 (2007) 312–318.
[12] G. Petruccia and M. Rosellini, Chlorine dioxide in seawater for fouling control and post-disinfection in potable waterworks, Desalination, 182 (2005) 283–291.
[13] S. Belfer, Y. Purinson, R. Fainshtein, Y. Radchenko and O. Kedem, Surface modification of commercial composite polyamide reverse osmosis membranes, J. Membr. Sci., 139 (1998) 175–181.
[14] J. Gilron, S. Belfer, P. Vaisanen and M. Nystrom, Effects of surface modification on antifouling and performance properties of reverse osmosis membranenes, Desalination, 140 (2001) 167–179.
[15] A.K. Ghosh, B.-H. Jeong, X. Huang and E.M.V. Hoek, Impacts of reaction and curing conditions on polyamide composite reverse osmosis membrane properties, J. Membr. Sci., 311 (2008) 34–45.
[16] N. Kim, D.H. Shin and Y.T. Lee, Effect of silane coupling agents on the performance of RO membranes, J. Membr. Sci., 300 (2007) 224–231.
[17] A. Fujumori, S. Chiba, N. Sato, Y. Abe and Y. Shibasaki, Surface morphological changes in monolayers of aromatic polyamides containing various N-alkyl side chains, J. Phys. Chem. B, 114 (2010) 1822–2835.
[18] D. Mukherjee, A. Kulkarni and W.N. Gill, Chemical treatment for improved performance of reverse osmosis membranes, Desalination, 104 (1996) 239–249.
[19] D. Rana and T. Matsuura, Surface modifications for antifouling membranes, Chem. Rev., 110 (2010) 2448–2471.
[20] A.P. Rao, S.V. Joshi, J.J. Trivedi, C.V. Devmurari and V.J. Shah, Structure-performance correlation of polyamide thin film composite membranes: effect of coating conditions on film formation, J. Membr. Sci., 211 (2003) 13–24.
[21] J. Yang, S. Lee, E. Lee, J. Lee and S. Hong, Effect of solution chemistry on the surface property of reverse osmosis membranes under seawater conditions, Desalination, 249 (2009) 148–161.
[22] J.E. Elliott, M. Macdonald, J. Nie and C.N. Bowman, Structure and swelling of poly(acrylic acid) hydrogels: effect of pH, ionic strength, and dilution on the crosslinked polymer structure, Polymer, 45 (2004) 1503–1510.
[23] S. Wu, J. Xing, C. Zheng, G. Xu, G. Zheng and J. Xu, Plasma modification of aromatic polyamide reverse osmosis composite membrane surface, J. Appl. Polym. Sci., 64 (1997) 1923–1926.
[24] M. Manttari, A. Pihlajamaki and M. Nystrom, Effect of pH on hydrophilicity and charge and their effect on the filtration efficiency of NF membranes at different pH, J. Membr. Sci., 280 (2006) 311–320.